

Influence of structure on the mechanical behavior of an agricultural clay soil

Robert Medjo Eko^{1*}, Claude Laguë²

(1. *University of Yaoundé I, Cameroon;* 2. *University of Ottawa, Canada*)

Abstract: A better understanding of soil mechanical properties is needed to assess soil compaction in clay soil. To fill that need, a research program was undertaken at Laval University, Quebec city, Canada to ultimately find better solutions in managing Sainte Rosalie clay compacted by liquid manure spreaders. The soil used for the investigation was collected from a field where soil compaction was monitored. It was statically compacted in loose and dense states to reflect the soil conditions above and below the plow pan. Tests on both saturated and unsaturated samples of Sainte Rosalie clay were then carried out. They were conducted within an isotropic stress state framework to analyze the mechanical behavior of the soil. Data gathered from the investigation show that different compaction states lead to different loading-collapse (LC) yield curves.

Keywords: isotropic state, suction, unsaturated soil, soil structure

Citation: Robert Medjo Eko, and Claude Laguë. 2012. Influence of structure on the mechanical behavior of an agricultural clay soil. *Agric Eng Int: CIGR Journal*, 14(4): 1–8.

1 Introduction

The mechanical behavior of aggregated soils is often associated with particular complexities due not only to their structure but also to extra strength components stemming from the aggregation and interparticle bonding (Koliqi, Vulliet, and Laloui, 2010). Delage and Lefebvre (1984) used mercury intrusion porosimetry and scanning electron microscopy to characterize the structure modification on non compacted clay induced by the mechanical loading under saturated conditions. They showed that, at a given stress increment during consolidation, only the largest pores collapse, and small pores are compressed when all of the macropores have been completely closed. Simms and Yanful (2001, 2002) investigated the effects of suction variation on the structure of a compacted unsaturated glacial till and noted a progressive rise of microporosity associated with macroporosity reduction as the suction increased. In a

later work, Simms and Yanful (2005) examined the hydromechanical coupling effects in unsaturated clayey soils and proposed a model to predict the overall volume change of the materials and the evolution of pore size distribution. Modeling the mechanical behavior of an unsaturated soil using the Basic Barcelona Model (Alonso, Gens, and Josa, 1990) shows that soil parameters such as slope of normal consolidation line ($\lambda(s)$) and swelling index ($\kappa(s)$) are affected by specific volume of the soil (Alonso et al., 1995), in other words they are affected by soil structure. As pointed out by Li (2005), some measure of soil structure should be taken into consideration to accommodate the effects of suction while studying the mechanical behavior of an unsaturated soil.

In this paper, the effect of structure on the limit state and loading collapse curves of a heavy agricultural clay soil prone to compaction is investigated through a comprehensive set of experiments. The soil samples were statically compacted in loose and dense states to reflect the soil density above and below the plow pan. The mechanical behavior of the soil was then analyzed using net mean stress and suction within triaxial and isotropic stress state frameworks. A comparison between

Received date: 2012-05-25 **Accepted date:** 2012-08-08

* **Corresponding author:** Robert Medjo Eko, PO Box 812, Department of Earth Sciences, Faculty of Science, University of Yaoundé I, Cameroon. Email: rmedjo@yahoo.com.

the mechanical behavior of loose and dense samples is finally carried out and explained.

2 Materials and methods

2.1 Soil physical characteristics

The soil under investigation was an agricultural soil named Sainte Rosalie clay. It was collected from Saint Simon, a small village located at 60 km East Montreal, Canada. The soil was dried for over 6 months in a soil bin at the Agri-Food Engineering Department, Laval University, Canada. It was then grounded and sieved through a 2 mm diameter mesh. The soil was later used in the various identification tests listed below.

2.1.1 Grain Size analysis

The result is plotted at Figure 1. The use of triangular textural classification chart shows that Sainte Rosalie clay is a heavy agricultural clay soil.

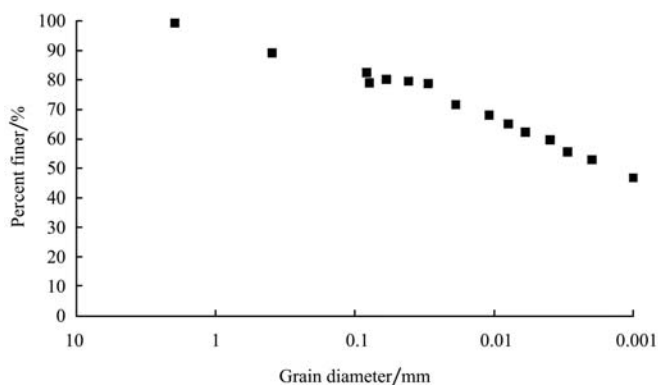


Figure 1 Grain size distribution of Sainte Rosalie clay

2.1.2 Standard proctor test

The test yielded an optimum water content of 24% and a maximum dry density of 1,585 kg m⁻³. Degree of saturation was 91%, which was pretty high compared to common degrees of saturation at optimum (Figure 2). This may stem from the presence of the organic content in the soil which was found to be 3.2%.

2.1.3 Atterberg limits

Liquid limit was 45% and Plastic limit was 24%. Plasticity Index was related to Liquid limit according to the following equation:

$$Ip = 0.85 (Wl - 19) \tag{1}$$

The above equation governs $Ip - Wl$ relationships of soils from Champlain Sea where Sainte Rosalie clay was collected (Leroueil, Tavenas, and Le Bihan, 1983). The

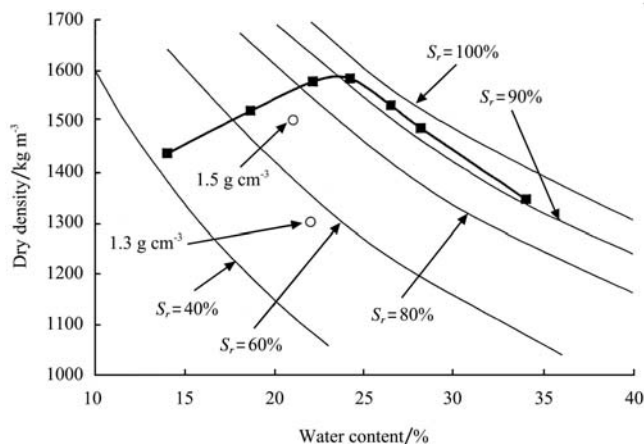


Figure 2 Compaction curve of Sainte Rosalie clay

relationship for Sainte Rosalie clay is very close to the general equation proposed by Casagrande for common soils. The latter is as follows:

$$Ip = 0.73 (Wl - 20) \tag{2}$$

2.1.4 Activity

Soil activity was found to be 0.40; it was concluded that Sainte Rosalie clay would not swell on wetting.

2.1.5 Specific weight

Specific weight of soil was 2.68; this figure was lower than common range of specific weights encountered in Champlain Sea. In effect, the latter range from 2.70 to 2.75 (Leroueil, Tavenas, and Le Bihan, 1983)

2.1.6 Soil-water characteristic curves

They were obtained using the filter paper method of soil suction measurement. The method is fully described in Chandler and Gutierrez (1986) Fredlund and Rahardjo (1993), and Marinho (1994). The soil-water characteristic curves derived for two soil dry densities (1.3 g cm⁻³ and 1.5 g cm⁻³) are plotted at Figure 3.

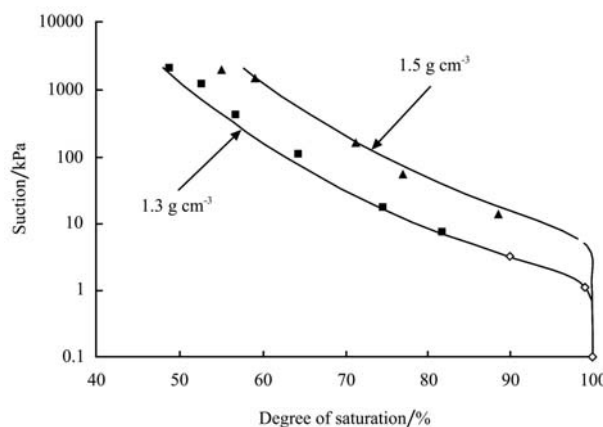


Figure 3 Soil water characteristic curves of loose and dense soil samples

2.2 Static compaction of soil samples

Soil samples for subsequent tests were compacted at 1.3 g cm^{-3} and 1.5 g cm^{-3} dry densities. The above soil densities represent common dry densities of soil layer in the agricultural region where Sainte Rosalie clay was collected. Early soil studies carried out in that region showed that common dry densities are 1.3 g cm^{-3} in the upper 25 cm of soil layer while it rises up to 1.5 g cm^{-3} in the following 25 cm of the same soil profile (De Kimpe and Mehuys, 1979; Chi et al., 1993). These soil dry densities result from soil compaction induced by farm equipment trafficking and soil management related to agricultural activities. The dry densities are compared with the standard Proctor result at Figure 2.

Two categories of samples have been processed:

- The first category was made of 3.81 diameter and 7.1 cm high samples; this sample category was intended to be used in triaxial tests.
- The second category was made of 2.54 cm high and 3.5 cm diameter samples; this sample category was intended to be used in soil suction measurement tests.

Samples of both categories were processed using a static compaction device. Water content during compaction of 1.3 g cm^{-3} samples was 22% while that of 1.5 g cm^{-3} samples was 21%. Water content on compaction was based on a survey conducted by Chi et al. (1993) on sites where Sainte Rosalie supports agricultural activities.

Samples for triaxial tests were compacted in a 3.81 cm diameter mold. They were compacted in 4 layers to ensure the best standard homogeneity. Each layer of 1.5 g cm^{-3} was compacted using a 240 kPa pressure while each of 1.3 g cm^{-3} was compacted using 120 kPa pressure. The device used for static compaction did not allow each layer to settle beyond a preset level upon compaction. This allowed samples to be compacted up to the desired dry density. Top of each layer was carefully scarified after placement. The best homogeneity along the interface joining two adjacent layers was obtained thanks to this process. After compaction, the mold was dismantled and the sample was collected.

2.3 Isotropic compression tests on saturated soil samples

The tests were carried out on saturated samples. The

procedure was done as follows: the sample was placed in a conventional triaxial cell. A 10 kPa all-round and 2 kPa back-pressures were both applied to the sample. This allowed occurrence of an 8 kPa gradient, which triggered water to circulate from bottom to top in the sample. Drainage on top of the sample was open at the beginning of the water circulation. It permitted the air in the sample to be driven out thanks to the incoming water. When first drops of water showed up, the drainage was shut off. Then all-round pressure and back pressure were both increased in steps of 25 kPa. Both pressures were maintained 3 to 4 hours at each step. More water was such allowed into the sample. Before increasing both pressures to the next step, sample level of saturation was first checked by computing the B Skempton parameter. It was found that B Skempton parameter reached 0.95 to 0.97 when all-round pressure and back pressure reached respectively 210 kPa and 202 kPa. The soil sample was therefore technically saturated. From this point, the all around desired pressure could be applied.

2.4 Isotropic compression tests on unsaturated soil samples

The tests were carried out only on unsaturated soil samples. Materials for testing unsaturated soil samples were the following: a double wall-triaxial cell was used to carry out triaxial tests. It allowed application of the "axis translation method" proposed by Hilf (1956). After soil sample was mounted in the triaxial cell, pore water pressure u_w equal to the atmosphere pressure was applied at the base and the top of the specimen through porous ceramics with an entry value of 500 kPa. The air pressure u_a was applied to the sample through a hole in the rubber membrane and a diffuser made of geotextile at the mid-height of the specimen. Such a set-up was chosen to decrease the drainage length and consequently the time necessary to achieve equilibrium during the different phases of the tests. The air pressure selected was equal to the desired matrix suction $s = u_a - u_w$. The cell pressure σ_3 selected was equal to the sum of air pressure and the desired net confining pressure ($\sigma_3 + u_a$). The vertical stress was applied by a triaxial compression frame during shear tests.

The vertical displacements of the sample were

measured externally with a deflectometer. The volume change of the pore water was measured with burettes connected to the cell base and the top of sample. In order to flush out any diffused air bubbles that formed under the porous stones, spiral grooves were connected to the base of the burette in a closed circuit of tubes with a peristaltic pump, allowing a gentle circulation of water under the stones and the flushing out of air bubbles.

The procedure applied during drained triaxial test on unsaturated soil was as follows: all the tests were performed under constant suction condition. At the beginning of the procedure, a net confining stress of 5 kPa was applied in the triaxial cell. The degree of saturation at that time was around 70% for the 1.5 g cm⁻³ samples and 55 % for the 1.3 g cm⁻³ samples. The air pressure was applied by steps of 10 kPa. Duration at each step was 15 min. To keep the piston applying axial load in contact with the sample, a 5 kPa axial stress in excess of the cell pressure was maintained during application of air pressure. When the air pressure corresponding to the desired suction was reached, the soil specimen was maintained under this condition until sample water content and air pressure came to equilibrium. In fact, during air pressure application, water was driven out of the sample. As long as drainage went on, it was the sign that the desired suction was not fully applied yet. It was considered that the desired suction was applied to the sample only when air pressure and sample water content reached equilibrium. The drainage took usually around 2 weeks for stabilization to occur (Figure 4). After stabilization, increments of σ_3 were applied up to the

desired confining pressure. During σ_3 increase, σ_1 was also increased in such a way that the 5 kPa axial stress in excess of the cell pressure was always maintained.

3 Experimental results

3.1 Material behavior under saturated condition

Isotropic compression. The results are plotted on a v-log p' diagram where p' is the effective stress (Figures 5 and Figure 6). Each of the two curves exhibits two approximately linear segments meaning that soil samples were overconsolidated. At Figure 5, the plot shows that sample of 1.3 g cm⁻³ yields at 30 kPa while sample of 1.5 g cm⁻³ yields at 70 kPa (Figure 6). The compression index (λ) varies from 0.17 to 0.13 when sample dry density varies from 1.3 g cm⁻³ to 1.5 g cm⁻³. This suggests that soil compressibility decreases when dry density increases. The rebound index (κ) also varies when soil dry density changes. The parameter κ varies from 0.040 to 0.012 when dry density varies from 1.3 g cm⁻³ to 1.5 g cm⁻³; which means that the slope κ in

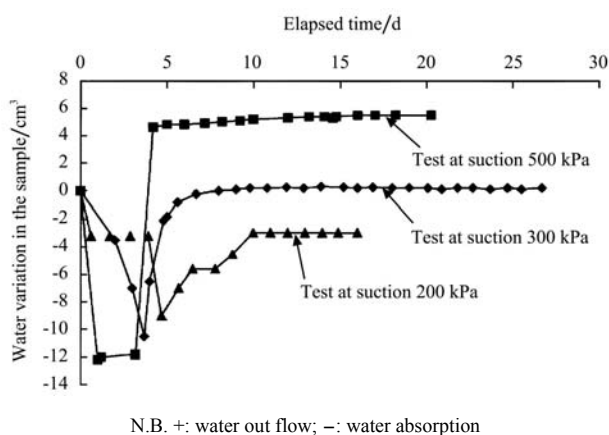


Figure 4 Water variation in the soil samples during suction application

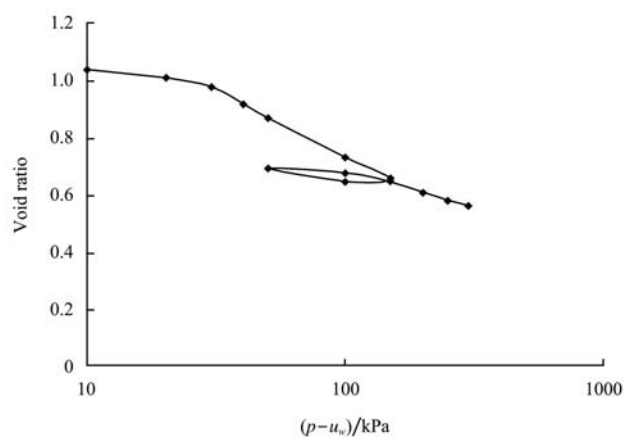


Figure 5 Isotropic compression of saturated loose soil sample

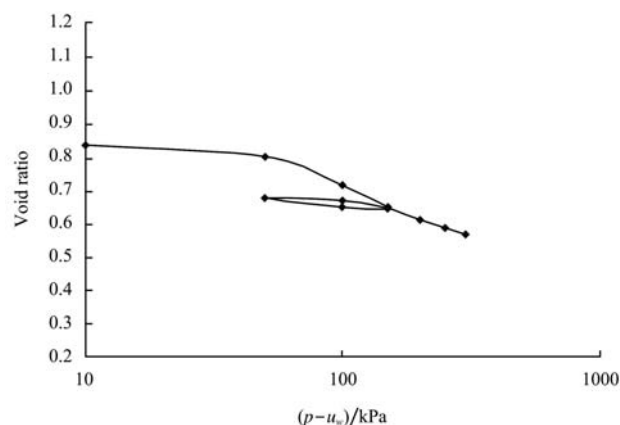


Figure 6 Isotropic compression of saturated dense soil sample

the elastic zone decreases when dry density increases. The change of κ with dry density can actually be considered as negligible given the value of the parameter.

3.2 Material behavior under unsaturated condition

This section deals with tests on both saturated and unsaturated soil conditions.

3.2.1 Isotropic compression

Tests were run at 300 kPa and 500 kPa suction. Once the desired suction was applied, an all-round pressure was progressively applied. Loading ratio of one-dimensional compression was used for this test but steps applied did not exceed 50 kPa. Steps over 10 kPa were applied by increments of 10 kPa. Duration at 10 kPa increment was 15 min. Once a 50 kPa step was reached, the pressure was maintained for 2 days to ensure both water exchange and volume changes. Four tests were carried out on the two categories of soil samples. Resulting curves are sketched at Figures 7 and Figure 8. Complete results of isotropic compression on both saturated and unsaturated soil samples are displayed in Table 3.

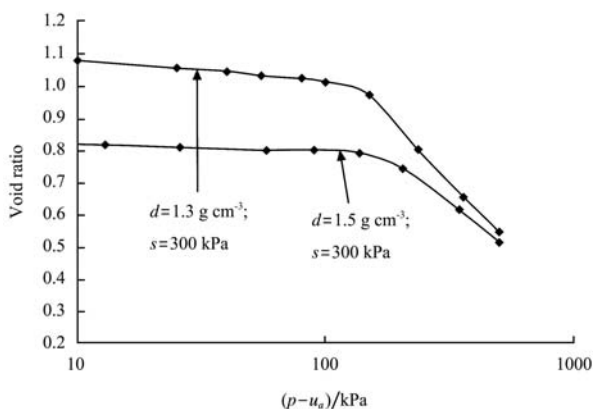


Figure 7 Isotropic compression of loose and dense soil samples at suction 300 kPa

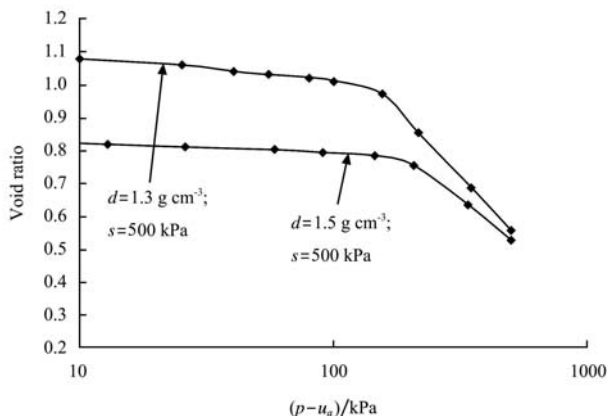


Figure 8 Isotropic compression of loose and dense soil samples at suction 500 kPa

Results show that the yield stress is closely related to the initial dry density. In other words a soil with a low initial dry density ends up with a low yield stress when isotropically compressed. Based on data in Table 3, it also appears that the yield stress increases with an increasing suction. It can be derived that the influences of suction and dry density are similar on soil strength: any increase of either factor increases the soils strength.

Table 3 Influence of suction and dry densities on isotropic yield stress

Dry density/g cm ⁻³	Suction	$\lambda(s)$	σ'_{iso}	$\kappa(s)$
1.30	0	0.17	30	0.040
1.30	300	0.33	130	0.025
1.30	500	0.31	150	0.031
1.50	0	0.13	70	0.012
1.50	300	0.24	170	0.010
1.50	500	0.22	190	0.012

Although data are limited, it is observed that both compression index $\lambda(s)$ and $\kappa(s)$ vary with suction (Figure 9 and Figure 10). Beyond suctions that correspond to optimum water content (s_{opt}), the variations of $\lambda(s)$ and $\kappa(s)$ are reversed.

Data in Table 3 are used to sketch the Loading Collapse (LC) model of the soil (Figure 11). The LC model relates yield stresses from isotropic compression to suctions at which compressions are performed. The procedure allows drawing yield surfaces over various soil suctions and dry densities. It can be observed that shapes of both curves are similar to those of Alonso, Gens, and Josa (1990).

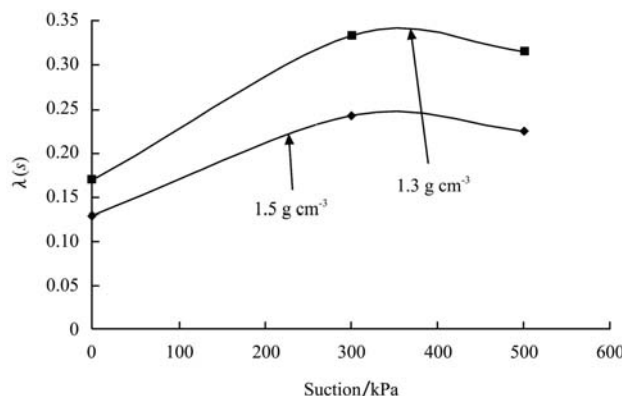


Figure 9 Variation of soil compressibility for loose and dense soil samples

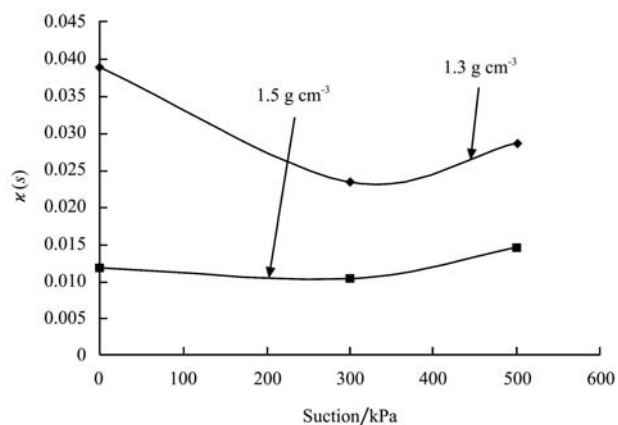


Figure 10 Variation of rebound index for loose and dense soil samples

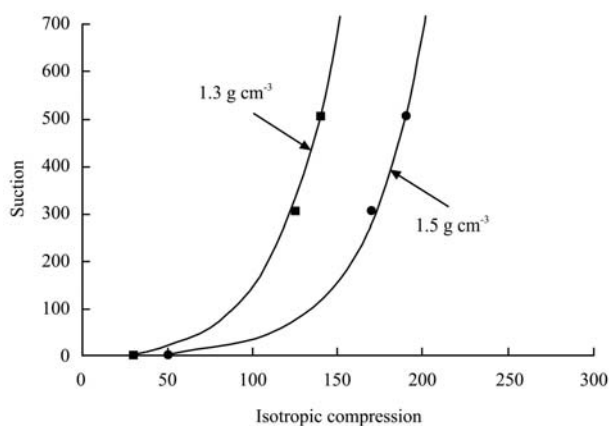


Figure 11 Loading-Collapse (LC) yield curves of loose and dense soil

In the LC model, the compressibility parameter ($\lambda(s)$) is expressed as a function of $\lambda(0)$ and two parameters β and r according to the following equation

$$\lambda(s) = \lambda(0)[(1-r)\exp(-\beta s) + r]$$

where, $\lambda(s)$ = soil compressibility at suctions; $\lambda(0)$ = soil compressibility at saturation; r = maximum soil stiffness; β = increase of soil stiffness with suction.

3.2.3 LC yield curves

The LC yield curves for dense and loose samples were produced from the yield points obtained from isotropic compression results (Figure 11). The shape of the LC curves is consistent with those proposed in Alonso, Gens, and Josa (1990) and in Estabragh, Javadi, and Boot (2004). The results show that over suctions, the yield stresses of dense samples are higher than those of loose samples. In other words the LC curve expands while Sainte Rosalie clay gets denser. It can therefore be stated that the difference in structure of Sainte Rosalie

clay located above and below the plow pan is reflected in the difference of LC curves.

4 Discussion

Figure 9 shows the variation of $\lambda(s)$ for dense and loose samples under various suctions. The value of $\lambda(s)$ for loose sample is about 1.4 times greater than the value for dense samples. The difference is kept nearly constant whatever the suction. It is observed that the higher the specific volume of Sainte Rosalie clay, the higher the compressibility. A look at the compaction curve of Sainte Rosalie clay shows that loose and dense samples were compacted almost at the same water content to represent the soil condition in the field. They ended up with different compressibility parameters $\lambda(s)$. This finding is consistent with the observation of Matyas and Radakhrishna (1968) who state that for unsaturated conditions, when two soil samples are compacted with the same water content but under two different compaction pressures, the denser sample will be less compressible than the loose sample.

The variation of $\lambda(s)$ from this investigation is similar to the variation of $\lambda(s)$ from Estabragh, Javadi, and Boot (2004). In effect, it is observed that $\lambda(s)$ values from this investigation decrease with increasing suctions for suctions greater than 300 kPa (80 kPa for Estabragh et al. (2004)). This is consistent with the model proposed by Alonso, Gens, and Josa (1990). However, for suctions lower than 300 kPa (80 kPa for Estabragh, Javadi, and Boot (2004)), $\lambda(s)$ values decrease as suctions are reduced to zero. This is no more consistent with the model of Alonso, Gens, and Josa (1990) which proposes that the slope of isotropic normal consolidation lines $\lambda(s)$ decreases monotonically with increasing suction from the saturated value $\lambda(0)$ to asymptotic value $r \lambda(0)$ at high suctions. The compressibility ($\lambda(s)$) of Sainte Rosalie clay reported above may be explained through the experimental results of Delage et al. (1996) and the observation of Ferber et al. (2008).

Beyond suction 300 kPa, aggregates of Sainte Rosalie clay behave according to the concept of rigid grains developed by Delage et al. (1996). Suctions higher than 300 kPa lead Sainte Rosalie aggregates (rigid grains) to

become stronger and stronger; which decreases soil compressibility ($\lambda(s)$) over increasing suctions. As a consequence, the slope of isotropic normal consolidation line $\lambda(s)$ decreases. The model of Alonso, Gens, and Josa (1990) is in agreement with this soil behavior.

In contrast, below suction 300 kPa, the variation of compressibility of Sainte Rosalie clay is consistent with the observation of Ferber et al. (2008). In effect, average pore sizes in loose and dense soils are respectively 145 μm and 37 μm according to DeKimpe and Mehuys (1979) who measured the pore sizes of this clayey soil in the field where compaction was monitored. It can be derived from their results that a substantial amount of pores of Sainte Rosalie clay are made up of macropores. Pores of this size are filled with air when the soil is in unsaturated condition (Ferber et al., 2008.) As suction is reduced from 300 kPa to zero, water gradually expels air contained in the macropores; which gradually decreases the soil compressibility ($\lambda(s)$). Therefore, the compressibility of Sainte Rosalie clay increases from $\lambda(0)$ up to the level where the microstructure change suggested by Delage et al. (1996) is observed. The model of Alonso, Gens, and Josa (1990) is no longer in agreement with this behavior. Ignoring the change of microstructure which takes place in the soil when suction increases from zero to higher values, may explain why the model of Alonso, Gens, and

Josa (1990) does not account for the reduction of $\lambda(s)$ when suction decreases from its highest value (300 kPa in this investigation and 80 kPa in Estabragh, Javadi, and Boot (2004)) down to zero.

5 Conclusions

The goal of the experimental investigation conducted here was to study the effect of structure on the mechanical behavior of an agricultural heavy clay soil. The experimental results show that the LC yield curve of the soil below the plow pan expand to greater extent than the corresponding curves for the soil above the plow pan. This fact mainly stems from agricultural activities carried out above the plow pan while soil gets denser below the plow pan. It was observed that soil densification which corresponds to the lowering of soil void ratio shifts the LC curve to the right.

For a given water content, the compression index $\lambda(s)$ decreases with increasing density. This aspect of the unsaturated soil behavior is not considered in the model proposed by Alonso, Gens, and Josa (1990) and Wheeler and Sivakumar (1995). Furthermore, there may be a microstructure change which reverses the variation of compression and rebound indices over the suctions. In this investigation, the point at which this microstructure change occurs was found to be around the optimum water content i.e. at suction 300 kPa.

References

- Adams, B.A., and D. Wulfsohn. 1996. Application of critical state and unsaturated soil mechanics principles to an agricultural soil. ASAE paper No 96-1065, *American Society of Agricultural and Biological Engineers*, St Joseph, MI.
- Al-Mukhtar, M. 1995. Macroscopic behavior and microstructural properties of a kaolinite clay under controlled mechanical and hydraulic state. In *Proceed of the 1st Int. Conf. on Unsaturated Soils*, Paris, Vol. 1, pp.3-9.
- Al-Mukhtar, M., N. Belanteur, D. Tessier, and S.K. Vanapalli. 1996. The fabric of a clay soil under controlled mechanical and hydraulic stress states. *Applied Clay Science*, 11 (2-4): 99-115.
- Alonso, E.E., A. Gens, and D.W. Hight. 1987. Special problem soils. General report. In *Proc. 9th Conference of Soil Mechanics and Foundation Engineering*, Dublin, 31 August-3September, 1987, Vol. 3, A.A Balkema, Rotterdam, The Netherlands, pp. 1087-1146.
- Alonso E.E., A. Gens, and A. Josa. 1990. A constitutive model for partially saturated soils. *Geotechnique*, 40(3): 405-430.
- Alonso, E.E, A. Lloret, , A. Gens, and D.Q. Yang. 1995. Experimental behavior of highly expansive double-structure clay. *Proceedings of the 1st International Conference on Unsaturated soils*. Paris, 6-8 Sept. 1995. Vol 1 edited by E.E. Alonso and P. Delage, A.A Balkema, Rotterdam, the Netherlands, pp. 11-16.
- Brustaert, W. 1968. The permeability of a porous medium determined from certain probability laws for pore size distribution. *Water Resour. Res.*, 4 (2): 425-434.

- Chandler, R.J., and C.I. Gutierrez. 1986. The filter paper method of suction measurement, *Geotechnique*, 36 (2): 265-268.
- Chi, L., S. Tessier, and C. Lague. 1993. Finite element prediction of soil compaction induced by various running gears. *Trans. of the ASAE*, 36 (3): 629-636.
- Delage, P., M. Audiguier, Y.J. Cui, and M.D. Howat. 1996. Microstructure of a compacted silt. *Canadian Geotechnical Journal*, 33 (1): 150-158.
- Delage, P., and G. Lefebvre. 1984. Study of the structure of a sensitive clay and of its evolution during consolidation. *Canadian Geotechnical Journal*, 21 (1): 21-35
- De Kimpe, C.R., and G.R. Mehuys. 1979. Physical properties of gley solic soils in the low lands of Québec. *Can. J. Soil Sc.* 59: 69-78.
- Estabragh, A.R., A.A. Javadi, and C. Boot. 2004. Effect of compaction on consolidation behaviour of unsaturated silty soil. *Can. Geotech. J.*, 41 (3):540-550.
- Ferber, V., J.C. Auriol, Y-J Cui, and J.P. Magnan. 2008. Wetting-induced volume changes in compacted silty clays and high-plasticity clays. *Can. Geotech. J.* 45: 252-265
- Fredlund, D.G., and H. Rahardjo. 1993. *Soil Mechanics for Unsaturated Soils*. John Wiley & sons, N.Y, 515 pp.
- Gardner, R. 1937. A method of measuring the capillary tension of soil moisture over a wide moisture range. *Soil Sc.*, 43 (4): 277-283.
- Gupta, S.C., and R.R. Allmaras. 1987. *Adv. Soil Sc.* 6, 65-100. (to author: please complete the issue number)
- Hilf, J.W. 1956. *An investigation of pore water pressure in compacted cohesive soils*. Technical Memorandum, No. 654, Bur. of Reclamations, U.S Department of Interior, Denver, Colorado.
- Kay, B.D. 1990. Rates of change of soil structure under different cropping systems. *Adv. Soil Sc.* 12, 1-41
- Keller, J. 1970. Sprinkler intensity and soil tilth. *Trans. ASAE*, 13 (6): 118-125.
- Koliji, A., L. Vulliet, and L. Laloui. 2010. Structural characterisation of unsaturated aggregated soil. *Can. Geotech. J.*, 47 (3): 297-311.
- Lambe, T.W. 1958. The engineering behavior of compacted clays. *J. Soil Mech. Found. Div., ASCE* 84, 1-35. (To author: please complete the issue number)
- Leroueil, S., F. Tavenas, and J.P. Le Bihan. 1983. Propriétés caractéristiques des argiles de l'Est du Canada. *Can Geotech. J.* 20 (4): 681-705.
- Li, X.S. 2005. Modeling of hysteresis response for arbitrary drying/wetting paths. *Computers and Geotechnics*, 32 (2): 133-137.
- Marinho, F.A.M. 1994. Shrinkage Behaviour of Some Plastic Soils. Ph.D. thesis, Imperial College, London.
- Marshall, T.J. 1962. The nature, development, and significance of soil structure. *Trans. Int. Soc. Sci. Comm. IV and V*, NZ, pp. 243-257
- Mc Kyes, E. 1985. *Soil cutting and tillage*. Elsevier, Amsterdam.
- Medjo Eko, R. 2005. Use of triaxial stress state framework to evaluate the mechanical behaviour of an agricultural clay soil. *Soil & Tillage Research*, 81 (1): 71-85.
- Or, D. 1996. Wetting induced soil structural changes: the theory of liquid phase sintering. *Water Resour. Res.* 32, 3041-3049.
- Pusch, R. 1982. Mineral water interactions and their influence on the physical behavior of highly compacted Na-bentonite. *Canadian Geotechnical Journal*, 19 (3): 381-387.
- Pusch, R., and T. Carlsson. 1985. The physical state of pore water of Na-smectite used as barrier component. *Engineering Geology* (Amsterdam), 21 (3/4): 257-265.
- Qi, Y., M. Al-Mukhtar, J-F Alcover, and F. Bergaya. 1996. Coupling analysis of macroscopic and microscopic behaviour in highly consolidated Na-laponite clays. *Applied Clay Science*, 11 (2-4): 185-197.
- Simms, P.H., and E.K. Yanful. 2001. Measurement and estimation of pore shrinkage and pore distribution in a clayey till during soil-water characteristic curve tests. *Can Geot. J.*, 38(4): 741-754.
- Simms, P.H., and E.K. Yanful. 2002. Predicting soil-water characteristics curves of compacted plastic soils from measured pore size distribution. *Geotechnique*, 52(4): 269-278.
- Simms, P.H., and E.K. Yanful. 2005. A pore network model for hydromechanical coupling in unsaturated compacted clayey soils. *Can. Geot. J.*, 42(2): 499-514.
- Sivakumar, V., and S.J. Wheeler. 2000. Influence of compaction procedure on the mechanical behavior of unsaturated compacted clay. Part 1. *Geotechnique*, 50 (4): 359-368.
- Sumner, M.E., and B.A. Stewart. 1992. *Soil Crusting: Chemical and Physical Processes*. *Advanced Soil Science*, Lewis, Boca Raton, FL, 372 pp.
- Sun, D., and D. Fredlung. 2008. Elasto-Plastic of unsaturated soils: an overview. *Proc. 12th Int. Conf. International Association for Computer Methods and Advances in Geomechanics (IACMAG)*, Goa, India.
- Tamari, S. 1984. Relations between pore space and hydraulic properties in compacted beds of silty loam aggregates. *Soil Technol*, 7 (1): 57-73.
- Wheeler, S.J., and V. Sivakumar. 1995. An elasto-plastic critical state framework for unsaturated soil. *Geotechnique*, 45 (1): 35-53.